Supporting Information

Bimetallic Zn/Co Telluride Spinel with Enhanced Metal-Tellurium Covalency for Efficient Water Oxidation

Shuowen Bo,[1,#] Qizheng An,[1,#] Yu Zhu,[1,#] Xiuxiu Zhang,[1] Yuhao Zhang,[1] Hui-Juan Wang,[3] Juguang Han,[1] Hui Su,[2,*] Qinghua Liu[1,*]

[1]*National Synchrotron Radiation Laboratory, University of Science and Technology of China, Hefei 230029, Anhui, P. R. China;*

[2]*Key Laboratory of Light Energy Conversion Materials of Hunan Province College, College of Chemistry and Chemical Engineering, Hunan Normal University, Changsha 410081, Hunan, P. R. China*

[3]*Experimental Center of Engineering and Material Science, University of Science and Technology of China, Hefei 230026 China*

[#]*These authors contributed equally: Shuowen Bo, Qizheng An, Yu Zhu.*

*E-mail: suhui@ustc.edu.cn; qhliu@ustc.edu.cn

Contents:

Materials and methods

Materials. Na_2TeO_3, $Co(NO_3)_2·6H_2O$, $CO(NH_2)_2$, NH_4F, $Zn(NO_3)_2$, C_2H_5OH. HCI were purchased from Sinopharm Chemical Reagent Co. Ltd. Commercial RuO_2 was purchased from Aladdin. All chemicals were used directly without further purification. Deionized water was used in all experiments.

Synthesis of $ZnCo_2Te_4$/NF electrocatalyst. The $ZnCo_2Te_4$ electrocatalysts was fabricated in four convenience designed steps, consisting of surface functionalization of 3D nickel foam (NF), high temperature hydrothermal precursors synthesis, hydrothermal vulcanization synthesis, and room temperature-conventional drying. First, the 3D nickel foam was cleaned by ultrasound vibration at 60 °C for 4 h, then nickel foam was washed with concentrated nitric and deionized water. Next, chemical ratios of 2 mmol $Zn(NO_3)_2·6H_2O$, 4 mmol $Co(NO_{3)2}·6H_2O$, 12 mmol $CO(NH_2)_2$, and NH_4F were mixed in 70 ml deionized water for 10 minutes, and the nickel foam and solution were put into a 45 ml polytetrafluoroethylene reactor, and the resulting mixed solution was dried at 120 ℃ for 8 h to obtain solid precursor, then the precursor was washed with deionized water and ethanol for 3 times. Next, the precursor was dried in a vacuum oven at 60 ℃ for 6 h. Subsequently, 0.05 mol of Na_2TeO_3 was dissolved into 40 ml deionized water to form the solution, then the nickel foam was put in the solution. The resulting solution was put into a 45 ml polytetrafluoroethylene reactor. The resulting solution was heated at 140 ℃ for 6 h , then washed three times with deionized water and ethanol. Finally, the resulting product was wiped with lint-free paper, then cooled at room temperature until dry naturally.

Morphology and structure characterizations.

The powder X-ray diffraction (XRD) patterns of samples were measured in a Philips X' Pert Pro Super X-ray diffractometer with Cu Kα radiation (λ = 1.54178 Å). Transmission electron microscopy (TEM), high-resolution transmission electron microscopy (HRTEM) and energy dispersive spectroscopy (EDS) were performed on a JEM-2100F microscope with an acceleration voltage of 200 kV. The field emission scanning electron microscopy (SEM) was acquired on a Gemini SEM 500 scanning electron microscope. X-ray photoelectron spectroscopy (XPS) spectra were acquired on an ESCALAB MKII with Mg Kα (hυ = 1253.6 eV) as the excitation source. The Co K-edge X-ray absorption near-edge spectra (XANES) were measured in National Synchrotron Radiation Laboratory (NSRL), which were measured in the total electron yield mode in a vacuum chamber (< 5 × 10^{-8} Pa). Inductively coupled plasma mass spectrometry (ICP-OES) was measured by using Inductively Coupled Plasma Optic Emission Spectrometer (Plasma Quad 3). Specific surface area (BET) was measured in a fully automatic surface area and porosity analyzer (Tristar II 3020M)

Electrochemical Measurements. All electrochemical measurements were performance in a three-electrode system by CHI760D electrochemical work station, operated with the self-supporting array grown on NF (the active area of 1×1 cm^{-2}) as the working electrodes, carbon electrode as the counter electrode, and the normal Hg/Hg_2Cl_2 electrode as the reference electrode. The three electrodes were immersed in 1M KOH as conductive media. All final potentials were converted to reversible hydrogen electrode (RHE) with the conversion E (vs. RHE) = E (vs. Hg/Hg_2Cl_2) + 0.245 V + 0.059 × PH. Linear sweep voltammetry (LSV) curves were obtained at a rate of 5 mV s^{-1} with IR correction after several cyclic voltammetry tests until stable. It is worth noting that electrochemical data were corrected for uncompensated series resistance R_s, which was determined through the open-circuit voltage, and we selected 90% IR compensation to obtain R_s. And the potential was determined by the following Eq: $E_{Corrected} = E_{Uncorrected} - I*R_S$

Mathematical formula for electrochemical measurements:

The roughness factor (RF) mathematical formula. The roughness factor (RF) was calculated by taking the estimated ECSA and S_{geo}, as following Eq.

$$RF=ECSA/ S_{geo}$$

The ECSA mathematical formula. The ECSA of the catalyst sample was calculated from the double layer capacitance according to the following Eq.

$$ECSA = C_{dl} / C_s$$

where C_s is the specific capacitance of the sample, and the typical value reported ranges between Cs= 0.02-0.06 mF/cm^2 in KOH, then we selected general specific capacitances of Cs=0.04 mF/cm^2.

based typical reported. Furthermore, to gain reliable data, we performed CV tests at a wide redox process-free window of 300 mV and suitable sweep speeds of 0.005, 0.01, 0.02, 0.05, 0.1, 0.5, 0.8, 1 V/s.

The J_{ECSA} mathematical formula. The definition of specific activity refers to the specific current density J_{ECSA}, which was calculated as according to the following Eq.

$$J_{ECSA} = J_{geo} /RF$$

The turnover frequency (TOF) and mass activity mathematical formula.

$$TOF = \frac{\text{the measured current density j}*NA*1000}{4*F*mol}$$

$$MA\ (\text{mass activity}) = \frac{j}{m}$$

The TOF and MA are activity metric reported in the electrocatalysis literature, which are depended on a given overpotential and the measured current density. It is assumed that every active metal atom of the catalyst participates in the reaction. The turnover frequency (TOF, s-1) can be calculated according to the equation: TOF =(j×A) / (4×F×M), where j is the current density at a given potential, A is the surface of the electrode, F is the faradaic constant, and M is the number of moles of active metal on

the electrode. The mass activity can be calculated according to the equation: Mass activity = (j × A) / m, where j is the current density at a given potential, A is the surface of the electrode, and m is the active metal loading mass on the electrode.

XAFS measurements.

The XAFS measurements of Co *K*-edge were carried out at the 1W1B station in the Beijing Synchrotron Radiation Facility (BSRF), China. The storage ring of BSRF was operated at 2.5 GeV with a maximum current of 250 mA. The beam from the bending magnet was monochromatized utilizing a Si (111) double-crystal monochromator. The data collection was carried out in transmission mode using ionization chamber for Co foil, and in transmission mode for Co_3O_4, CoOOH, $ZnCo_2Te_4$.

***In-situ* SRIR measurement.**

In-situ synchrotron radiation IR measurements were made at the infrared beamline BL01B of the National Synchrotron Radiation Laboratory (NSRL, China), and we performed electrochemical tests through a homemade top-plate cell to obtain better signal data. Specifically, in order to reduce the loss of infrared light and eliminate the effect of vibration absorption of water molecules, the catalyst electrode was tightly pressed against the ZnSe crystal window with a micron-scale gap. Attentively, during the *in-situ* SRIR measurements, the infrared signal is very sensitive to water molecules and it is easily disturbed. To obtain improved-infrared signal-to-noise ratio (SNR), we pressed the electrode and window to control the thickness of the water film on the micron scale. To avoid signal differences caused by sample shedding, infrared spectra were collected after a constant potential was applied to the catalyst electrode for 5 min. Before each systemic OER measurement, the background spectrum of the electrocatalyst electrode was acquired without applied voltage and the measure potential ranges of the OER were 1.2–1.6 V with an interval of 0.1 V.

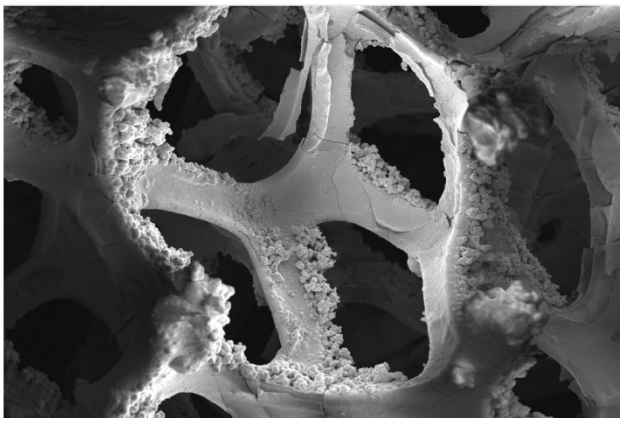

Fig. S1 The SEM image of catalyst on nickel foam

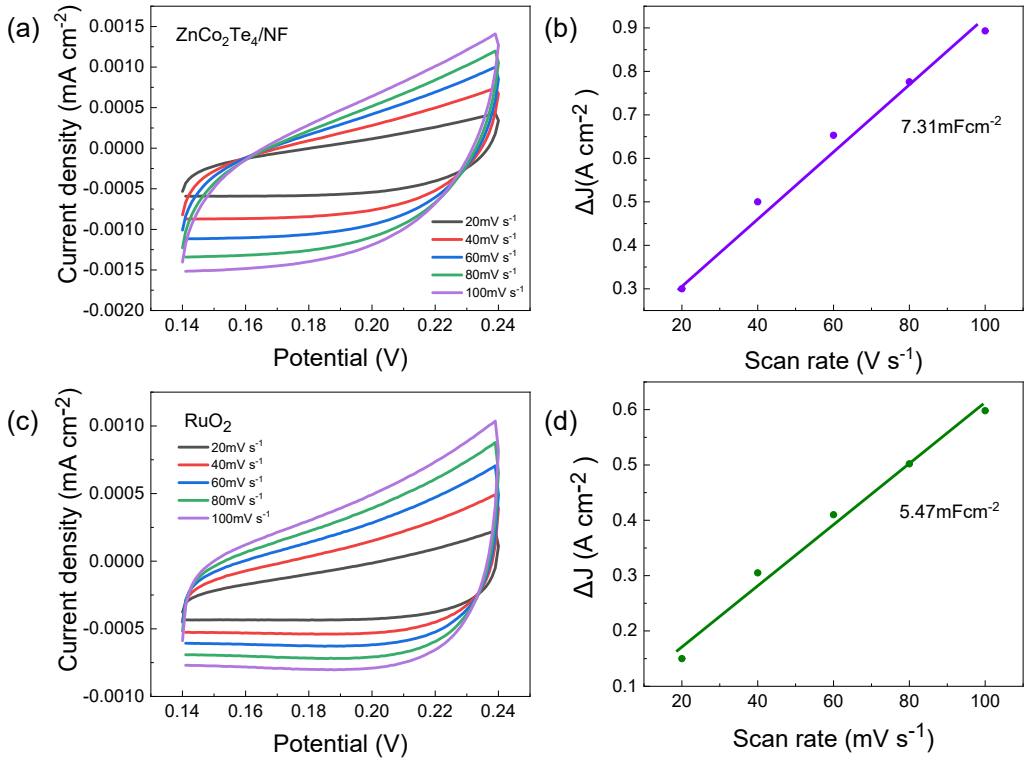

Fig. S2 Double-layer capacitance (C_{dl}) measurements. (a) and (c) CVs were conducted in a non-Faradaic region at the following scan rate: 20, 40, 60, 80, 100 mV s^{-1}. (b) and (d) The difference in charging currents variation at a potential plotted against scan rate for estimation of double-layer capacitance.

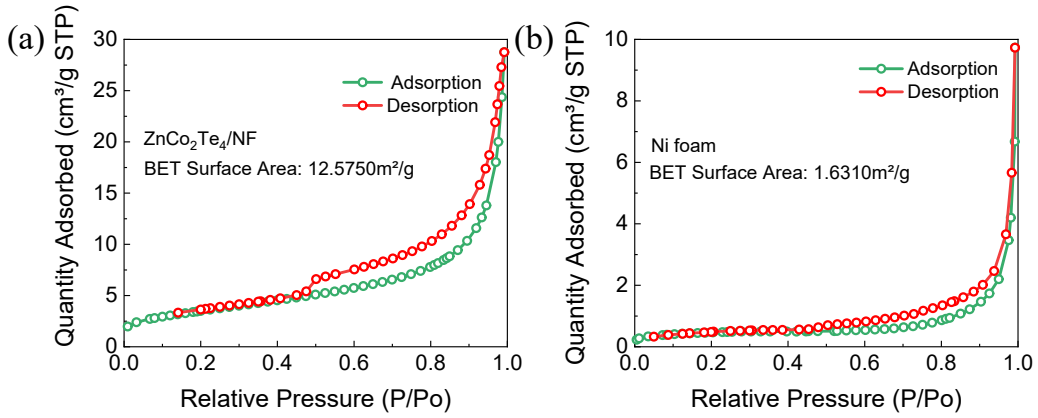

Fig. S3 Isotherm adsorption curve and specific surface area of (a) $ZnCo_2Te_4$/NF and T*he BET result shows that $ZnCo_2Te_4$/NF catalyst（Fig. S2a） possesses the high specific surface area. In order to avoid the influence of NF, we carry out the BET test of pure NF as well, and the result is displayed in supporting information as Fig. S2b from which the specific surface area is 1.6310 m^2/g, suggesting the high specific surface area originating the $ZnCo_2Te_4$ catalyst, not the NF.*

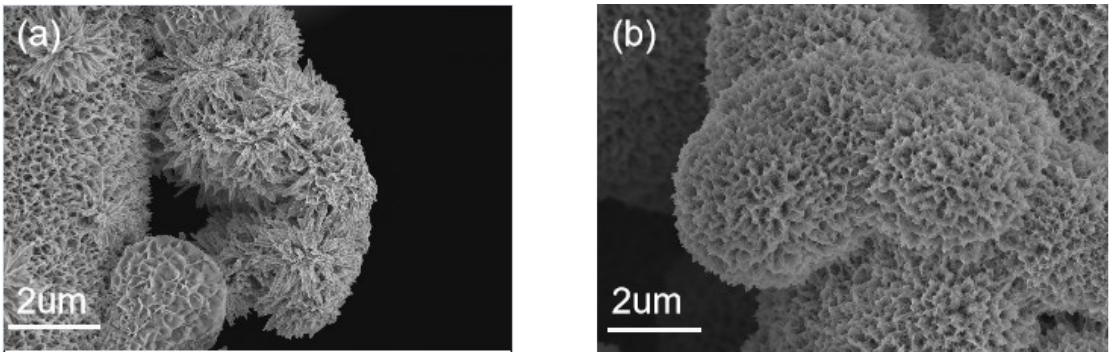

Fig. S4 (a) The SEM image before OER reaction and (b) SEM image after OER reaction

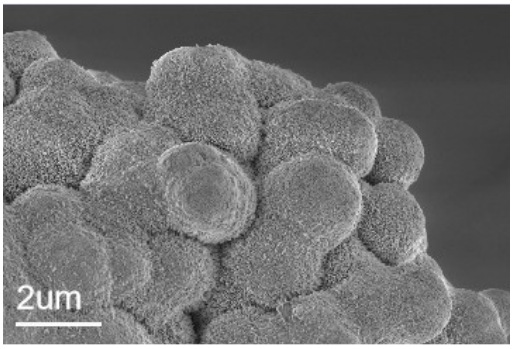

Fig. S5 The SEM image after 50h durability test

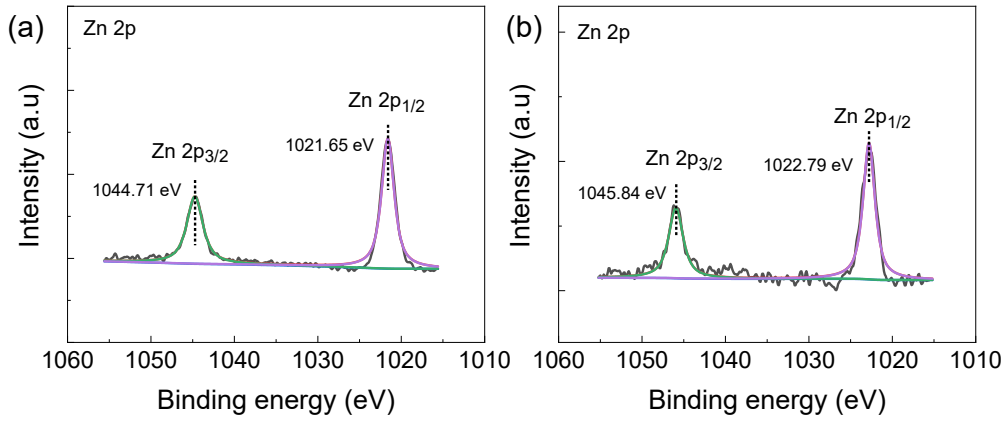

Fig. S6 The Zn 2p XPS survey spectra of $ZnCo_2Te_4$/NF electrocatalysts before and after OER

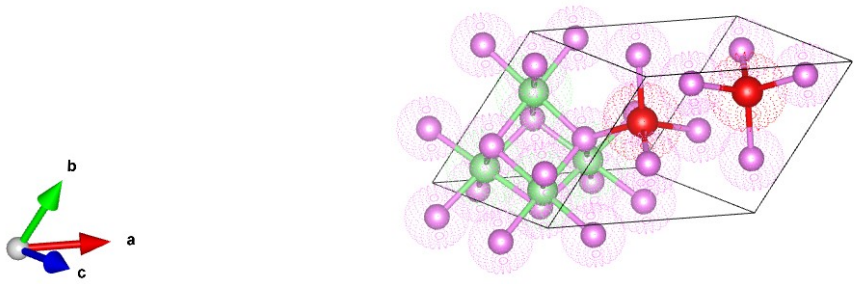

Fig. S7 The Crystal structure diagram of $ZnCo_2Te_4$

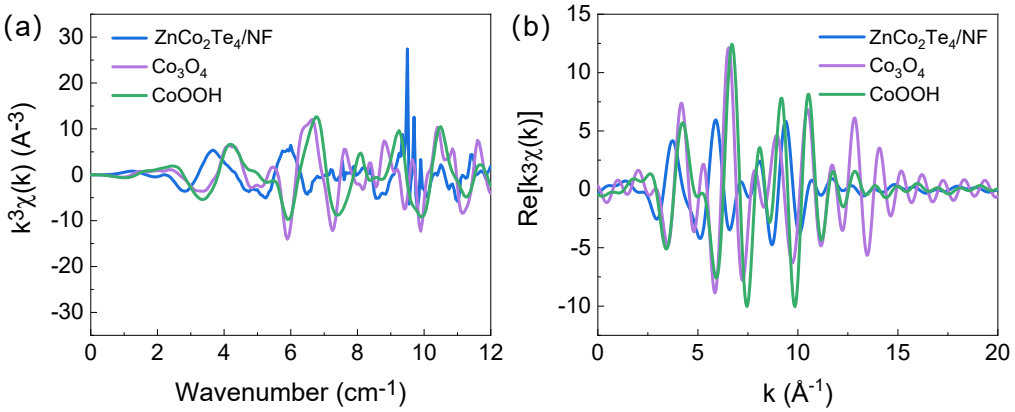

Fig. S8 The Co K-edge k space and q space oscillation curves for $ZnCo_2Te_4$/NF

(a)  (b) 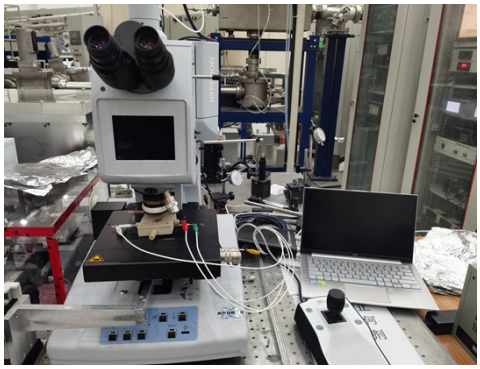

Fig. S9 Optical images of (a) XAS and (b) Operando SR-FTIR measurement.

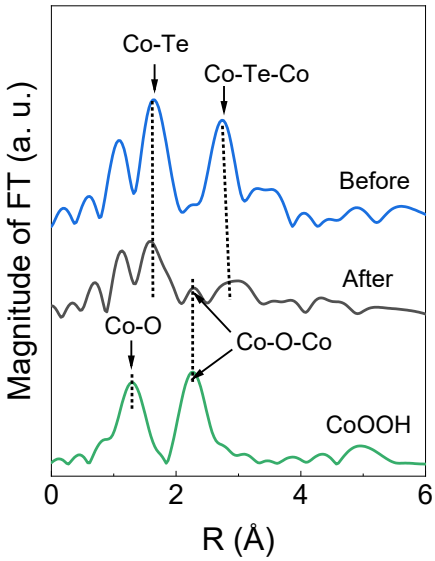

Fig. S10 Corresponding k^3-weighted Fourier transform (FT) spectra of $ZnCo_2Te_4$/NF before and after OER reaction and reference sample CoOOH.

Importantly, covalent bonds can serve as a bridge for electron transfer between Co and Te to facilitate the reaction. In order to further ensure whether Co-Te could maintain during the reaction, we carry out the ICP and XAFS experiments. Noted that the dissolution of Co^{3+} is slight detected over 10h (Tables S3), suggesting the Co-Te covalency bonding is not broke. For more directly demonstrating the presence of Co-Te in the reaction, XAFS results of catalyst after reaction is analyzed (Fig. S10) from which the evident signal of Co-Te appears after the reaction. These evidences strongly illustrates that the strong covalent bond contributing to the enhancement of OER performance accompanies the whole reaction process

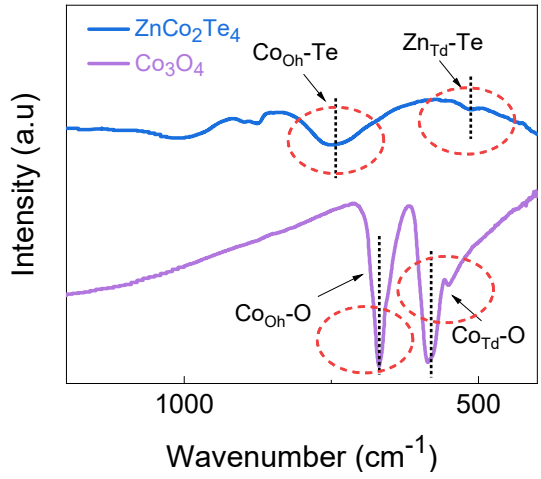

Fig. S11 The infrared spectroscopy of $ZnCo_2Te_4$, Co_3O_4.

Fourier infrared spectroscopy (Fig. 2b) detects the signal of Zn-Te and Co-Te bondings, suggesting the existence of covalent bonds in $ZnCo_2Te_4$/NF. In order to clear the real activity origin, it is necessary *to identify the effect of Zn-Te bonding. With the stronger Lewis acidity, Zn ions would more easily dissolve than Co ions. Inspired by this principle, we employ the inductively coupled plasma atomic emission spectroscopy analysis, and the results are displayed in Table N1. The rapid dissolution of Zn sites means Zn-Te bondings are hard to maintain, and the reinforced effect originating from Zn-Te is not sufficient.*

Tables.S1 ICP-OES results of $ZnCo_2Te_4$

Samples	Zn (wt%)	Co(wt%)	Te (wt%)
$ZnCo_2Te_4$	9.4	17.07	73.51

Table S2. Comparison of alkaline OER performance for $ZnCo_2Te_4$/NF as well as other electrocatalysts reported in the literatures.

Catalysts	Media	Performance	Reference
$ZnCo_2Te_4$/NF	1 M KOH	E_{over}=370mV@100mA cm^{-2}	This work
g-Co_3O_4	1 M KOH	E_{over}=354mV@100mA cm^{-2}	[1]
Ir-$NiCo_2O_4$	1 M KOH	E_{over}=500mV@100mA cm^{-2}	[2]
$CuCo_2O_4/Ti_3C_2T_x$	1 M KOH	E_{over}=440mV@100mA cm^{-2}	[3]
$NiCo_2O_4$@Ni-MOF	1 M KOH	E_{over}=340mV@100mA cm^{-2}	[4]
$CoFe_2O_4$	1 M KOH	E_{over}=300mV@100mA cm^{-2}	[5]
m-$NiCo_2O_4$	1 M KOH	E_{over}=383mV@100mA cm^{-2}	[6]
$Co_{2-x}V_xO_4$	1 M KOH	E_{over}=280mV@100mA cm^{-2}	[7]
MNFO NS/IF	1 M KOH	E_{over}=281mV@100mA cm^{-2}	[8]
$MnFe_2O_4$	1 M KOH	E_{over}=330mV@100mA cm^{-2}	[9]

Table S3 ICP-OES results of $ZnCo_2Te_4$ catalyst during OER process

Metal Concentration	1h	2h	5h	7h	10h
Zn^{2+}	5.6wt%	13.3wt%	19.8wt%	21.1wt%	23.2wt%
Co^{3+}	0.98wt%	1.07wt%	1.23wt%	1.35wt%	2.42wt%

Reference

1. L. Qi, M. Wang and X. Li, *CrystEngComm*, 2021, **23**, 7928-7931.
2. H.-J. Lee, D.-H. Park, W.-J. Lee, S.-B. Han, M.-H. Kim, J.-H. Byeon and K.-W. Park, *Applied Catalysis A: General*, 2021, **626**.
3. S. Ghorbanzadeh, S. A. Hosseini and M. Alishahi, *Journal of Alloys and Compounds*, 2022, **920**.
4. Z. Dai, X. Du and X. Zhang, *International Journal of Hydrogen Energy*, 2022, **47**, 17252-17262.
5. B. Debnath, S. Parvin, H. Dixit and S. Bhattacharyya, *ChemSusChem*, 2020, DOI: 10.1002/cssc.202000932.
6. A. Amirzhanova, N. Akmanşen, I. Karakaya and Ö. Dag, *ACS Applied Energy Materials*, 2021, **4**, 2769-2785.
7. C. Jiang, J. Yang, X. Han, H. Qi, M. Su, D. Zhao, L. Kang, X. Liu, J. Ye, J. Li, Z.-X. Guo, N. Kaltsoyannis, A. Wang and J. Tang, *ACS Catalysis*, 2021, **11**, 14884-14891.
8. Y. Peng, L. Sun, X. Yue and S. Huang, *ACS Applied Energy Materials*, 2022, **5**, 15239-15246.
9. M. Chen, N. Kitiphatpiboon, C. Feng, Q. Zhao, A. Abudula, Y. Ma, K. Yan and G. Guan, *Applied Catalysis B: Environmental*, 2023, **330**.